

Electromagnetic calorimeter for Belle II

This content has been downloaded from IOPscience. Please scroll down to see the full text.

2015 J. Phys.: Conf. Ser. 587 012045

(<http://iopscience.iop.org/1742-6596/587/1/012045>)

View the [table of contents for this issue](#), or go to the [journal homepage](#) for more

Download details:

IP Address: 131.169.4.70

This content was downloaded on 29/01/2016 at 22:52

Please note that [terms and conditions apply](#).

Electromagnetic calorimeter for Belle II

Belle-ECL¹, V Aulchenko^{1,5}, A Bobrov^{1,5}, A Bondar^{1,5}, B G Cheon², S Eidelman^{1,5}, D Epifanov⁶, Yu Garmash^{1,5}, Y M Goh², S H Kim², P Krokovny^{1,5}, A Kuzmin^{1,5}, I S Lee², D Matvienko^{1,5}, K Miyabayashi⁴, I Nakamura³, V Shebalin^{1,5}, B Shwartz^{1,5*}, Y Unno², Yu Usov^{1,5}, A Vinokurova^{1,5}, V Vorobjev^{1,5}, V Zhilich^{1,5}, V Zhulanov^{1,5}

¹ Budker Institute of Nuclear Physics SB RAS, Novosibirsk 630090, Russia

² Hanyang University, Seoul 133-791, Korea

³ High Energy Accelerator Research Organization (KEK), Tsukuba 305-0801, Japan

⁴ Nara Womens University, Nara 630-8506, Japan

⁵ Novosibirsk State University, Novosibirsk 630090, Russia

⁶ Department of Physics, University of Tokyo, Tokyo 113-0033, Japan

E-mail: * shwartz@inp.nsk.su

Abstract. The electromagnetic calorimeter of the BELLE II detector for experiments at Super B-factory SuperKEKB is briefly described. The project of the calorimeter upgrade to meet severe background conditions expected at the upgraded KEK B factory is presented.

1. Introduction

Experiments with the Belle detector [1] at KEKB B-factory [2], energy-asymmetric collider with high luminosity, were conducted from 1999 until 2010. In these experiments the world highest luminosity of the collider, $2 \times 10^{34} \text{ cm}^{-2} \text{ s}^{-1}$, was achieved that provided a basis to obtain ample results in several fields of particle physics. Although the most known Belle achievements concern the CP symmetry violation in the quark sector, very important results were also obtained in the heavy quarkonium spectroscopy, tau lepton decays and two-photon physics.

The Belle detector is a forward/backward asymmetric detector with high vertex resolution, precise magnetic spectrometry, very good calorimetry and sophisticated particle identification ability. It should be stressed that high energy resolution and detection efficiency for photons in a wide energy range is extremely important since one third of B-decay products are π^0 's and other neutral particles providing photons. Thus, a calorimeter able to detect photons in a energy range from 20 MeV to 4 GeV with high characteristics, is a very important part of the detector. The CsI(Tl) scintillation crystals were chosen as a material for the Belle calorimeter due to their high light output, short radiation length, good mechanical properties and moderate price. During more than 10 years of operation electromagnetic crystal calorimeter (ECL) of the Belle detector demonstrated its high quality and performance [4].

Initiated by the success of the KEKB/Belle experiment, the new advanced project, KEKB II/Belle II, was accepted. The KEKB II luminosity will exceed the previous one by about 40 times. Belle II should have considerably higher performance than Belle. This upgrade will open exciting possibilities in a search and study of new physics phenomena in the heavy quarkonia, lepton flavour violation in tau decays as well as in other particle physics fields.



Content from this work may be used under the terms of the [Creative Commons Attribution 3.0 licence](https://creativecommons.org/licenses/by/3.0/). Any further distribution of this work must maintain attribution to the author(s) and the title of the work, journal citation and DOI.

The first priority of the electromagnetic crystal calorimeter (ECL) upgrade is the calorimeter electronics modification following the general strategy of the Belle upgrade. The main idea is to shorten the shaping time from 1 μ sec to 0.5 μ sec and to use a pipe-line readout with waveform analysis.

The potential improvement at this way is limited by the long scintillation decay time of CsI(Tl) – 1 μ sec. Then for further improvement we consider the next stage of upgrade with a replacement of the slow CsI(Tl) crystals in endcaps to fast pure CsI scintillation crystals. This work is at the R&D stage now.

2. Belle/Belle II electromagnetic calorimeter

The Belle II detector project is described in the Technical Design Report [3]. Schematic view of the Belle II detector (top half) in comparison to the previous Belle detector (bottom half) is presented in Fig. 1.

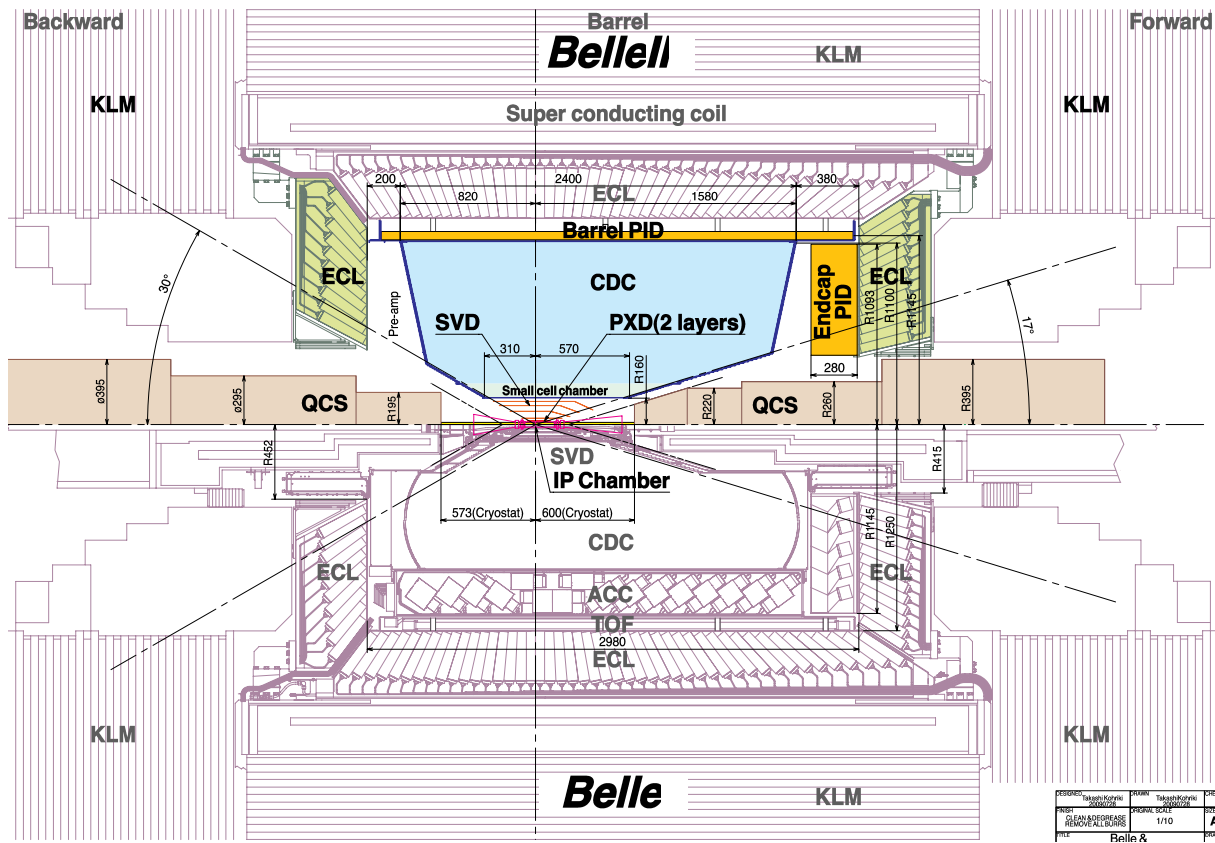


Figure 1. Schematic view of the Belle II detector (top half) in comparison to the previous Belle detector (bottom half).

The main tasks of the calorimeter are:

- detection of γ -quanta with high efficiency,
- precise determination of the photon energy and coordinates,
- electron/hadron separation,
- K_L detection together with KLM,
- generation of the proper signal for trigger,

- on-line and off-line luminosity measurements.

The electromagnetic calorimeter (ECL) consists of a 3 m long barrel section with an inner radius of 1.25 m and the annular endcaps at $z = 2.0$ m (Forward part) and $z = -1.0$ m (Backward part) from the interaction point. The calorimeter covers the polar angle region of $12.4^\circ < \theta < 155.1^\circ$ except two gaps $\sim 1^\circ$ wide between the barrel and endcaps.

The barrel part has a tower structure projected to the vicinity of the interaction point. It contains 6624 CsI(Tl) elements of 29 types. Each crystal is a truncated pyramid of the average size about $6 \times 6 \text{ cm}^2$ in cross section and 30 cm ($16.2X_0$) in length. The endcaps contain altogether 2112 CsI crystals of 69 types. The total number of the crystals is 8736 with a total mass of about 43 tons.

Each crystal is wrapped with a layer of 200 μm thick Gore-Tex porous teflon and covered by the 50 μm thick aluminized polyethylene. For light readout two $10 \times 20 \text{ mm}^2$ Hamamatsu S2744-08 photodiodes are glued to the rear surface of the crystal via an intervening 1 mm thick acrylite plate. The LED attached to the plate can inject the light pulses to the crystal volume to control the optical condition stability. A preamplifier is attached to each photodiode providing two independent output lines from each crystal. These two pulses are summed at the shaper board. For the electronics channel control the test pulses are fed to the inputs of the preamplifier. The average output signal of the crystals measured by calibration with cosmic rays is about 5000 photoelectrons per 1 MeV while a noise level is equal to about 200 keV. The energy resolution for photons, $\sigma E/E$, slightly changed from about 2.5% at 100 MeV to 1.7% at 5 GeV.

However, the experiment at SuperKEKB with a luminosity up to $8 \times 10^{35} \text{ cm}^{-2}\text{s}^{-1}$ puts new, severe requirements on the detector. Since KEKB collider is an e^+e^- machine with circulating beams up to 3–4 A, an obvious concern is a probable degradation of the crystal parameters due to a high radiation dose. The measured integrated dose absorbed by Belle ECL crystals by summer 2009 (i.e at integrated luminosity 900 fb^{-1}) is about 100 rad for the barrel part and about 400 rad in the most loaded part of the endcaps. The light output of the crystals is around 7% in the barrel and up to 13% in the endcap parts close to the beam pipe. These results are in a good agreement with previous measurements of the crystal radiation hardness [5]. Since these studies show the loss of the light output to be less or about 30% at 3.6 krad, an increase of the absorbed dose by one order of magnitude will not provide serious problems.

Another effect of the radiation background is the increase of the dark current of photodiodes induced by the neutron flux. At present the increase of the dark current in the barrel part is not substantial, less than 10 nA, while it is rather large in the endcap calorimeter – up to 200 nA. Thus, at the further high luminosity, we may encounter some problems caused by the high dark current.

The issue we have to treat more carefully is so called pile up noise caused by the soft background photons with average energy of about $1 \lesssim \text{MeV}$. The fluctuation of the number of these photons coming during the integration time contributes to the total noise level. The noise level, σ , measured at the luminosity of $L = 10^{34} \text{ cm}^{-2}\text{s}^{-1}$ already approaches to 1 MeV in the end caps that substantially exceeds the electronics noise.

High-energy photon background produces random clusters in the calorimeter. At present each event contains in average 6 background clusters (3 in barrel and 3 in the both endcaps) of the energy exceeding 20 MeV. We can expect 10 times high rate at Belle II which will produce a huge combinatorial background at the event reconstruction unless we upgrade calorimeter seriously.

3. ECL electronics upgrade

The main idea of the ECL electronics upgrade is to shorten the shaping time and to use a pipeline readout with waveform analysis. The shaping time becomes 0.5 μs and a counter signal is digitized continuously with 0.5 μs clock interval. Initiated by the trigger pulse, 16 points

within the signal are fit to the signal shape function $F(t)$: $F(t) = A_0 \times f(t - t_0)$ where A_0 is a pulse height and t_0 is an event time. The signal shape function, $f(t)$, is evaluated from separate measurements. Both amplitude (A_0) and time (t_0) are obtained by the on-line shape fit:

$$\chi^2 = \sum_{i,j} (A_i - F(t_i)) S_{ij}^{-1} (A_j - F(t_j)), \quad (1)$$

where A_i is an amplitude at the time t_i and S_{ij} - covariance matrix.

Time information allows to suppress the fake clusters by 7 times by rejecting wrong time clusters. At the described scheme the pileup noise will be reduced by a factor 1.5

A block diagram of the new ECL electronics is presented in Fig. 2. At least in the first years

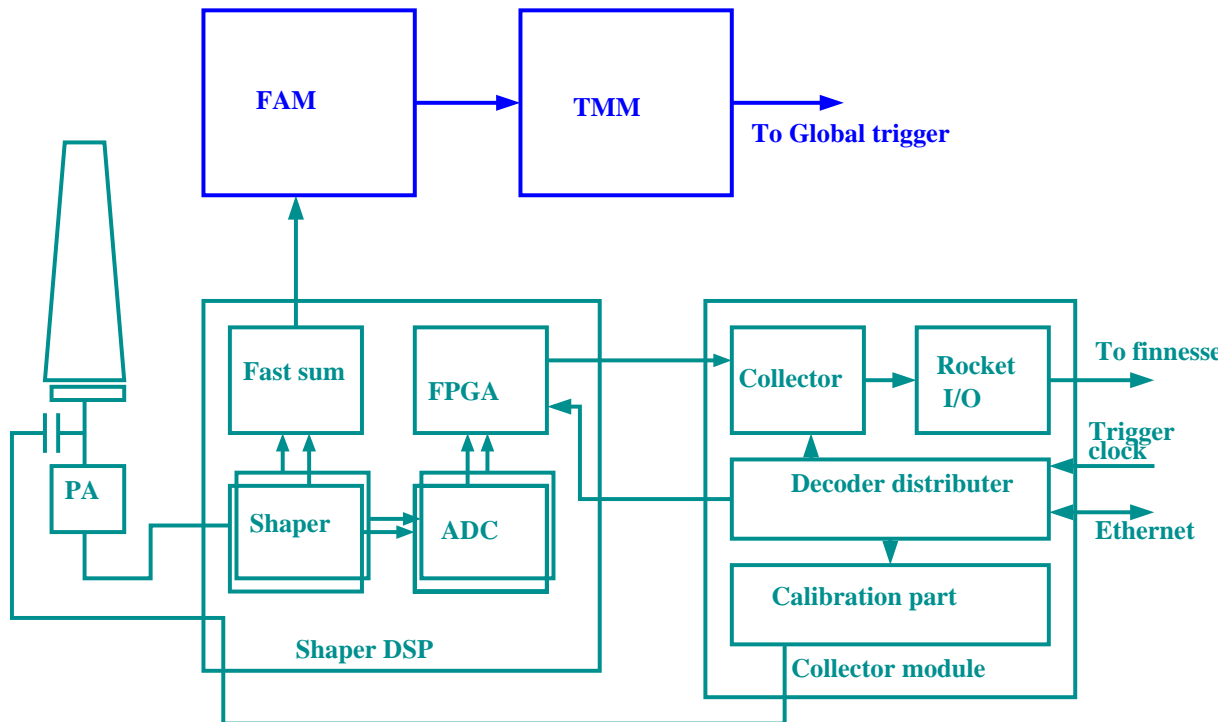


Figure 2. Block diagram of ECL electronics to read out CsI(Tl) crystals at Belle-II experiment.

of Belle-II experiment, the existent CsI(Tl) crystals, both in the barrel and endcaps will be used together with the same PIN-Photo-diodes, preamplifiers and the cables to reach the shaper are planned to be used. The Shaper-QT modules used for the Belle ECL are replaced by the Shaper-DSP modules.

New shaper-digitizer boards will keep the density of 16 channels per module. Each channel contains a shaping amplifier CR-(RC)⁴ ($\tau_s = 0.5\mu\text{s}$) and 18-bit flash ADC (Analog Devices AD7641) which digitizes the signal with 2 MHz clock frequency. The ADC data are read out by the digital processor realized in the XILINX FPGA. The data processing is initialized by the trigger signal and yields three parameters (amplitude, time and a quality of the data) which are calculated according to the algorithm described above.

The data from the Shaper-DSP are sent to the Collector module which packs the data of 8-12 Shaper-DSP modules and sends this by ROCKET-I/O line to COPPER FINNESSE module of Belle II DAQ. The collector module contains also a part for the test pulse generation to calibrate the response of the channel.

Each Shaper-DSP module also includes fast shaping ($\tau_d = 0.2 \mu\text{s}$) and gain adjustment circuits per each channel for a trigger output. A fast analog sum signal which is combined with 16 gain-corrected fast shaping channels is delivered to the FAM (Flash-ADC trigger Module) where a trigger cell signal is generated after comparing with a threshold ($\sim 100 \text{ MeV}$). These trigger cell signals are collected and processed by the TMM (Trigger and Monitoring Module) where ECL subtrigger arguments are formed and sent to GDL.

The simplified block diagram of the pulse analyzing part is shown in Fig. 3. The digital processor is built in XILINX FPGA XC3S1500-FG456 which has enough resources to realize waveform analysis in real time. The SDRAM chips are used to store precomputed coefficients for the digital signal processor (DSP). The idea of the waveform analysis algorithm is following.

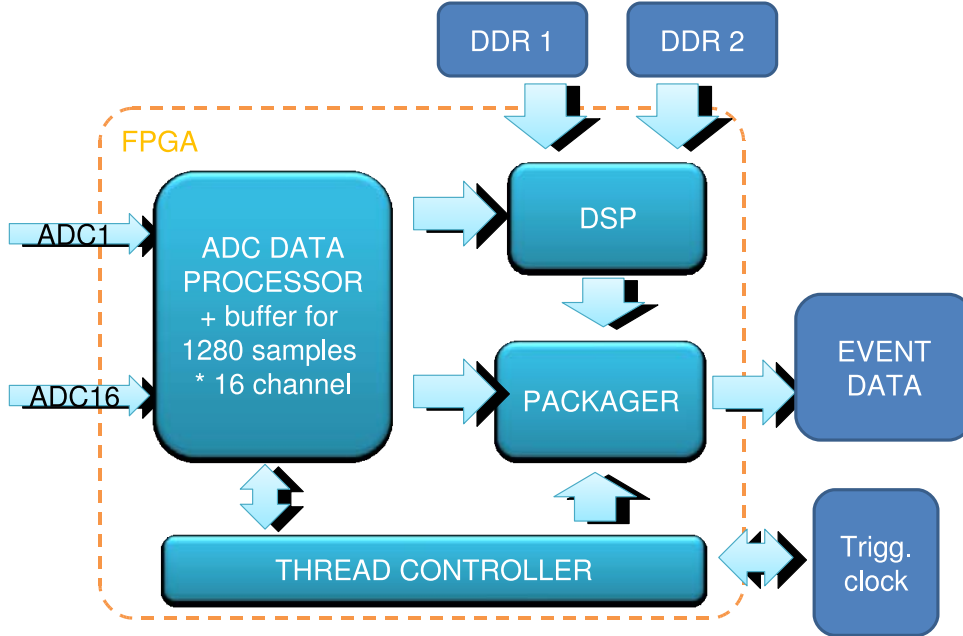


Figure 3. Schematic diagram of digital circuit realized by the FPGA for the energy and time measurements.

First, the signal function $f(t)$ as well as its derivative $f'(t)$ are tabulated to obtain the tables of values $f_{ki} = f(t_{ki}) = f(k\delta t + i\Delta t)$, where Δt is the digitizing interval, and δt is the timing bin width of tabulation that must be much smaller than Δt , i and k are the corresponding bin indexes. Linearizing $A_0 f(t)$ in Eq. 1

$$A f(t_{ki} - t_0) = A_0 f(t_{ki}) - t_0 A_0 f'(t_{ki}) = A_0 f_{ki} + B f'_{ki},$$

we can rewrite Eq. 1 taking a pedestal p into account:

$$\chi^2 = \sum_i (A_i - A_0 f_{ki} - B f'_{ki} - p) (S^{-1})_{ij} (A_j - A_0 f_{kj} - B f'_{kj} - p). \quad (2)$$

The minimization of this functional is equivalent to the linear system solution:

$$\sum_{i,j} f_{ki} S_{ij}^{-1} (A_j - A_0 f_{kj} - B f'_{kj} - p) = 0 \quad A_0 = \sum_i \alpha_i^k A_i$$

$$\sum_{i,j} f'_{ki} S_{ij}^{-1} (S^{-1})_{ij} (A_j - A_0 f_{kj} - B f' k j - p) = 0 \Rightarrow B = \sum_i \beta_i^k A_i, t_0 = -B/A_0$$

$$\sum_{i,j} S_{ij}^{-1} (S^{-1})_{ij} (A_j - A_0 f_{kj} - B f' k j - p) = 0 \quad p = \sum_i \gamma_i^k A_i \quad (3)$$

where α_i^k , β_i^k , γ_i^k are expressed via tabulated value f_{ki} , f'_{ki} and covariation matrix S^{-1} . Three parameters are obtained by the solution: amplitude (A_0), peak time (t_0) and pedestal (p). The obtained t_0 allows to calculate new k -index for the next iteration. Three iterations are enough for the convergence of the solution. For the first iteration the trigger time is used as the initial pulse time. As one can see from Eq. 3 one division and multiply-and-accumulate (MAC) operations are needed at each iteration. Fixed-point arithmetic and precomputed array of coefficients (α_i^k , β_i^k , γ_i^k) are sufficient to realize the algorithm at FPGA in real time computing.

For some fraction of data both input information (at 16 or 32 points) are sent to DAQ together with output parameters for algorithm and electronics monitoring.

4. Current status

The current activity on the ECL upgrade is going in several directions.

- New electronics production and tests.
- ECL trigger modules (FAM and TMM) development.
- On-line luminosity moniror development.
- Development of the software for the calorimeter DAQ and optimisation of the signal processing in the DSP.
- R&D works towards further endcap calorimeter upgrade.

By now the Shaper-DSP and Collector modules has been developed and these are in a production stage. All 432 barrel Shaper-DSP modules were delivered to KEK and tested with the specially developed test bench. In the test procedure following characteristics of the modules are checked: signal shape; FAM signal shape; slope and linearity; electronics noise level; FPGA logic and the attenuation range. All tested modules showed the proper characteristics. The measured nonlinearity of the Shaper-DSP is less than 2×10^{-3} within the full 260 000 bins of the ADC range.

All 144 Sh-DSP modules for the endcap parts will be delivered to KEK and test during 2014.

After the Great Japan Earthquake of 2011 it was important to check the status all channels of the barrel calorimeter (endcap parts were dismounted by that time). A special stand-alone test setup containing 12 Shaper DSP (prototype) modules, collector and FAM modules in one VME crate controlled by PC were prepared. Then all 6624 channels were tested batch by batch using cosmic ray particles. Fortunately all channels appeared to be operable.

5. Pure CsI in the endcaps

The drastic way to improve the characteristics of ECL is a replacement of the slow CsI(Tl) crystals with faster ones, at least in the end cap parts of the calorimeter. In the frame of this option pure CsI crystals of the same shape and size as the presently used CsI(Tl) counters are proposed for the end cap. The advantages of this crystal are a short scintillation decay time and moderate cost in comparison to other fast scintillation crystals. Since physical properties of the pure CsI are the same as CsI(Tl) the present sizes of the calorimeter element as well as the mechanical structure can be kept. Properties of pure CsI in comparison with CsI(Tl) scintillation crystals are listed in the Table 1.

However, the light output of pure CsI crystals is approximately ten times lower than that of doped crystals. Thus, to keep the electronics noise value at the same level one needs to use photo

detectors with internal gain. A suitable solution is to use vacuum photopentodes (PP), i.e. PM tubes with three dynodes. Since pure CsI emission wavelength is about 300 nm the photosensor should be UV sensitive. Such a device of 2-inch diameter with a low output capacity $C \approx 10$ pF has been recently developed by the Hamamatsu Photonics. The low capacity is important since the noise level depends on this value. The new developed PP have a quantum efficiency of about 20-25% and internal gain factor of 120-200 at zero magnetic field which reduces by factor 3.5 times for the $B=1.5$ T (see Fig. 4).

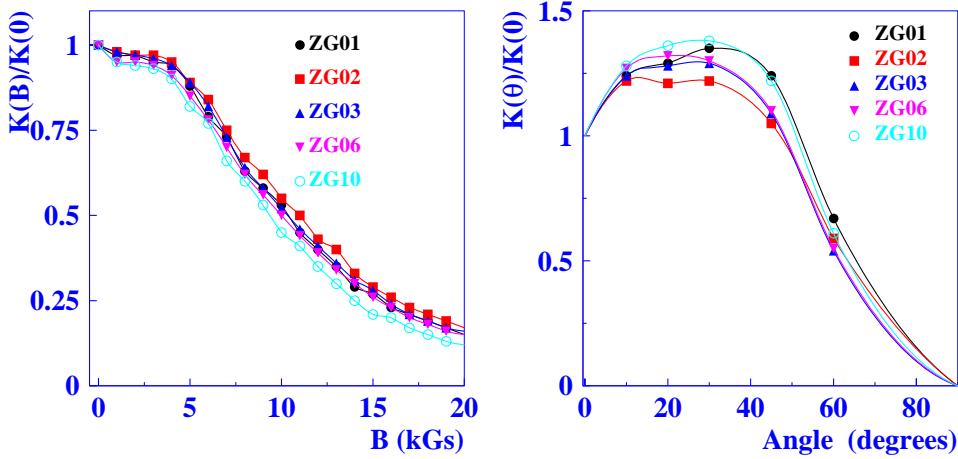


Figure 4. The photopentode gain in dependence on the magnetic field and the angle device axis to the field direction for the five devices.

The electronics channel will be built in the same general line as for the barrel part (see previous Section). The shaping and digitizing part is proposed to be implemented on VME boards. Each VME board contains 16 channels. Each channel includes a differential receiver, CR-(RC)⁴ shaper with shaping time $\tau = 30$ ns and two 14-bits fast flash ADCs. Usage of two ADCs allows to have effective 18-bit digitization for a full dynamical range. Digitization of the signals from the shaper outputs will be performed under the control of the common clock of 43 MHz. The digitized data are processing in FPGA to obtain the amplitude(A_0), time(t_0) and quality bits(Q) for each hit.

In the tests with the counter and electronics prototypes we obtained the signal of about $2 \cdot 10^4$ electrons per 1 MeV (without magnetic field) and the noise of about 900 electrons. These results can be extrapolated to the 1.5 T magnetic field as 6000 e/MeV and 200 keV of the noise energy equivalent.

Shorter scintillation decay time with matched shorter shaping time of the electronics channel allows to suppress the pile-up noise by a factor of about 5.5 in comparison to the present end cap parts of the calorimeter. The fake photon rate is suppressed by a factor of more than 100 due

Table 1. Properties of pure CsI and CsI(Tl) scintillation crystals

	ρ , g/cm ³	X_0 , cm	λ_{em} , nm	$n(\lambda_{em})$	N_{ph}/MeV	τ_d , ns	dL/dT , %/° 20°C
pCsI	4.51	1.85	305	2.0	2000	20/1000	- 1.3
CsI(Tl)	4.51	1.85	550	1.8	52000	1000	0.4

to a good timing providing by the mentioned scheme. Thus, even in the case of 20 times larger background the resulting fake rate is expected to be lower than in the current barrel calorimeter.

We performed a study of radiation hardness of the full size pure CsI crystals produced in Kharkov (Ukraina). In these study 14 full size crystals were irradiated by the wide gamma beam with the average energy of about 1 MeV generated by the 1.5 MeV electron accelerator ELV-6 at BINP. The absorbed dose increased step by step up to 14 krad. The most of the crystals (11) showed a light output reduction less than 20% while for 3 crystals the light output drops to 25-30% Thus, we consider the radiation hardness of the pure CsI crystals as acceptable for Belle II encaps.

The beam test with 20 pure CsI crystals coupled with PP and electronics provided waveform analysis was carried out at BINP photon beam [6].

The photon beam is produced by the Compton back scattering of the laser photons by the high energy electron beam circulating in the VEPP-4M storage ring. The resulting Compton spectrum is approximately uniform with a sharp edge corresponding to the maximum energy $\omega = 4\gamma^2\omega_0/(1 + 4\gamma\omega_0/m_e)$, where γ is a electron beam relativistic factor, ω_0 is the energy of the laser photon and m_e – electron mass. The energy resolution can be studied both by analyzing of the smearing of the Compton edge of the measured spectrum using the scattered electron tagging system.

Measured energy resolution (Fig. 5) is consistent with the CsI(Tl) ECL energy resolution [7] and MC predictions. The time resolution better than 1 ns for energy more than 20 MeV has been obtained.

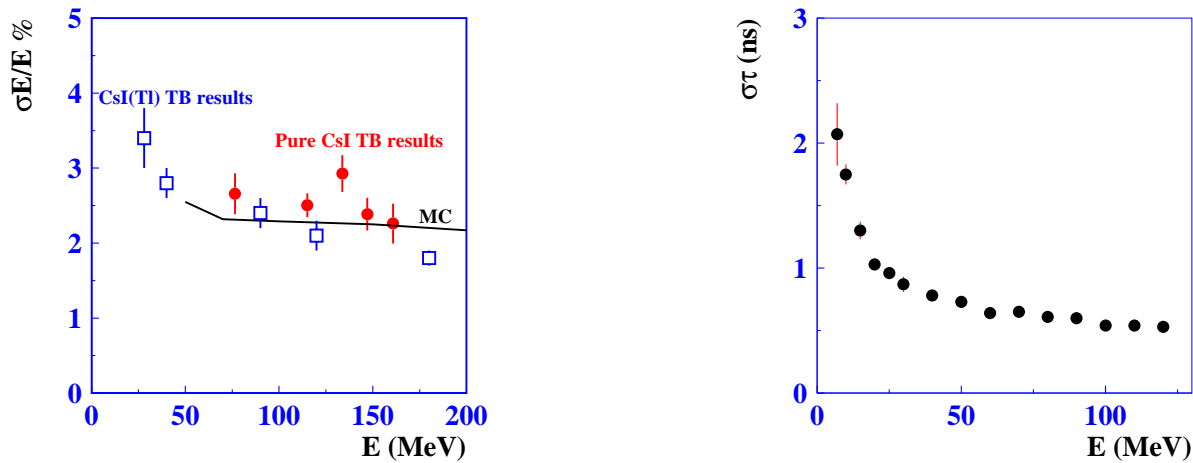


Figure 5. Energy (left plot) and time (right) resolution for photons obtained at the beam test (circles) and the results from beam test of the Belle ECL CsI(Tl) prototype [7] (squares).

6. Conclusion

- To keep good performance of the calorimeter at high background conditions of the Belle II experiment we upgrade the calorimeter electronics. This work is in progress. Most of the modules are produced and tested. The tests demonstrated proper performance of the new electronics.
- R&D works on the endcap calorimeter based on pure CsI counters with modified electronics is going on. This modification should provide drastic suppression both pile-up noise as and fake clusters rate in the endcaps.

7. Acknowledgments

We acknowledge support from the Ministry of Education, Culture, Sports, Science, and Technology (MEXT) of Japan; National Research Foundation of Korea and the Ministry of Education and Science of the Russian Federation

References

- [1] Abashian A *et al* . 2002 *Nucl. Instr. and Meth.*, A **479** 117
- [2] Kurokawa S *et al* . 2003 *Nucl. Instr. and Meth. A* **499** 1
- [3] Abe T *et al* . 2010 Belle II technical design report, KEK Report 2010-1
- [4] Cheon B G *et al* . 2002 *Nucl. Instr. and Meth. A* **494** 548
- [5] Kazui K *et al* . 1997 *Nucl. Inst. and Meth. A* **394** 46
Beylin D M *et al* . 2005 *Nucl. Inst. and Meth. A* **541** 501
- [6] Shwartz B 2009 *Nucl. Inst. and Meth. A* **598** 220
- [7] Ikeda H *et al* . 2000 *Nucl. Instrum. and Meth. A* **441** 401